Article

Molecular Engineering of Organic Sensitizers for Dye-Sensitized Solar Cell Applications

Daniel P. Hagberg, Jun-Ho Yum, HyoJoong Lee, Filippo De Angelis, Tannia Marinado, Karl Martin Karlsson, Robin Humphry-Baker, Licheng Sun, Anders Hagfeldt, Michael Grätzel, and Md. K. Nazeeruddin

J. Am. Chem. Soc., **2008**, 130 (19), 6259-6266 • DOI: 10.1021/ja800066y • Publication Date (Web): 18 April 2008

J|A|C|S
ARTICLES

Published on Web 04/18/2008

Molecular Engineering of Organic Sensitizers for Dye-Sensitized Solar Cell Applications

Daniel P. Hagberg,[†] Jun-Ho Yum,[§] HyoJoong Lee,[§] Filippo De Angelis,[||] Tannia Marinado,[‡] Karl Martin Karlsson,[†] Robin Humphry-Baker,[§] Licheng Sun,*[,†] Anders Hagfeldt,*[,‡] Michael Grätzel,[§] and Md. K. Nazeeruddin*[,§]

Organic Chemistry and Physical Chemistry, Center of Molecular Devices, Royal Institute of Technology, Teknikringen 30, 10044 Stockholm, Sweden, Laboratory for Photonics and Interfaces, Institute of Chemical Sciences and Engineering, School of Basic Sciences, Swiss Federal Institute of Technology, CH-1015 Lausanne, Switzerland, and Istituto CNR di Scienze e Tecnologie Molecolari (ISTM), c/o Dipartimento di Chimica, Università di Perugia, Via Elce di Sotto 8, I-06123, Perugia, Italy

Received January 4, 2008; E-mail: lichengs@kth.se; hagfeldt@kth.se; mdkhaja.nazeeruddin@epfl.ch

Abstract: Novel unsymmetrical organic sensitizers comprising donor, electron-conducting, and anchoring groups were engineered at a molecular level and synthesized for sensitization of mesoscopic titanium dioxide injection solar cells. The unsymmetrical organic sensitizers 3-(5-(4-(diphenylamino)styryl)thiophen-2-yl)-2-cyanoacrylic acid (D5), 3-(5-bis(4-(diphenylamino)styryl)thiophen-2-yl)-2-cyanoacrylic acid (D7), 5-(4-(bis(4-methoxyphenylamino)styryl)thiophen-2-yl)-2-cyanoacrylic acid (D9), and 3-(5-bis(4,4′-dimethoxydiphenylamino)styryl)thiophen-2-yl)-2-cyanoacrylic acid (D11) anchored onto TiO_2 and were tested in dye-sensitized solar cell with a volatile electrolyte. The monochromatic incident photon-to-current conversion efficiency of these sensitizers is above 80%, and D11-sensitized solar cells yield a short-circuit photocurrent density of 13.90 ± 0.2 mA/cm^2, an open-circuit voltage of 740 ± 10 mV, and a fill factor of 0.70 ± 0.02, corresponding to an overall conversion efficiency of 7.20% under standard AM 1.5 sun light. Detailed investigations of these sensitizers reveal that the long electron lifetime is responsible for differences in observed open-circuit potential of the cell. As an alternative to liquid electrolyte cells, a solid-state organic hole transporter is used in combination with the D9 sensitizer, which exhibited an efficiency of 3.25%. Density functional theory/time-dependent density functional theory calculations have been employed to gain insight into the electronic structure and excited states of the investigated species.

Introduction

Dye-sensitized solar cells (DSCs) have attracted significant attention as low-cost alternatives to conventional semiconductor photovoltaic devices.[1–10] These cells are composed of a wide band gap TiO_2 semiconductor deposited on a transparent conducting substrate, an anchored molecular sensitizer, and a redox electrolyte. Ruthenium sensitizers have shown very impressive solar-to-electric power conversion efficiencies, reaching 11% at standard AM 1.5 sun light.[11,12] Several groups, including ours, have developed metal-free organic sensitizers and obtained efficiencies in the range of 4−8%.[13–16] The critical factors that influence sensitization are the excited-state redox potential, which should match the energy of the conduction band edge of the oxide, light excitation associated with vectorial electron flow from the light-harvesting moiety of the dye toward the surface of the semiconductor surface, conjugation across the donor and anchoring groups, and electronic coupling

[†] Organic Chemistry, Royal Institute of Technology.
[‡] Physical Chemistry, Royal Institute of Technology.
[§] Swiss Federal Institute of Technology.
[||] CNR-ISTM, Perugia.

(1) Nazeeruddin, M. K. *Coord. Chem. Rev.* **2004**, *248*, 1161.
(2) Asbury, J. B.; Ellingson, R. J.; Gosh, H. N.; Ferrere, S.; Notzig, A. J.; Lian, T. *J. Phys. Chem. B* **1999**, *103*, 3110–3119.
(3) Park, N.-G.; Kang, M. G.; Kim, K. M.; Ryu, K. S.; Chang, S. H.; Kim, D.-K.; Van de Lagemaat, J.; Benkstein, K. D.; Frank, A. J. *Langmuir* **2004**, *20*, 4246–4253.
(4) Heimer, T. A.; Heilweil, E. J.; Bignozzi, C. A.; Meyer, G. J. *J. Phys. Chem. A* **2000**, *104*, 4256–4262.
(5) Saito, Y.; Fukuri, N.; Senadeera, R.; Kitamura, T.; Wada, Y.; Yanagida, S. *Electrochem. Commun.* **2004**, *6*, 71–74.
(6) Qiu, F. L.; Fisher, A. C.; Walker, A. B.; Peter, L. M. *Electrochem. Commun.* **2003**, *5*, 711–716.
(7) Kamat, P. V.; Haria, M.; Hotchandani, S. *J. Phys. Chem. B* **2004**, *108*, 5166–5170.
(8) Bisquert, J.; Cahen, D.; Hodes, G.; Ruehle, S.; Zaban, A. *J. Phys. Chem. B* **2004**, *108*, 8106–8118.
(9) Figgemeier, E.; Hagfeldt, A. *Int. J. Photoenergy* **2004**, *6*, 127–140.
(10) Furube, A.; Katoh, R.; Yoshihara, T.; Hara, K.; Murata, S.; Arakawa, H.; Tachiya, M. *J. Phys. Chem. B* **2004**, *108*, 12588–12592.
(11) Nazeeruddin, M. K.; De Angelis, F.; Fantacci, S.; Selloni, A.; Viscardi, G.; Liska, P.; Ito, S.; Bessho, T.; Grätzel, M. *J. Am. Chem. Soc.* **2005**, *127*, 16835–16847.
(12) M.Grätzel, J. *Photochem. Photobiol. A* **2004**, *164*, 3–14.
(13) Hara, K.; Sato, T.; Katoh, R.; Furube, A.; Ohga, Y.; Shinpo, A.; Suga, S.; Sayama, K.; Sugihara, H.; Arakawa, H. *J. Phys. Chem. B* **2003**, *107*, 597–606.
(14) Horiuchi, T.; Miura, H.; Sumioka, K.; Uchida, S. *J. Am. Chem. Soc.* **2004**, *126*, 12218–12219.
(15) Kim, S.; Lee, J. K.; Kang, S. O.; Ko, J.; Yum, J.-H.; Fantacci, S.; De Angelis, F.; DiCenso, Md., D.; Nazeeruddin, K.; Grätzel, M. *J. Am. Chem. Soc.* **2006**, *128*, 16701–16707.
(16) Hagberg, D. P.; Edvinsson, T.; Marinado, T.; Boschloo, G.; Hagfeldt, A.; Sun, L. *Chem. Commun.* **2006**, 2245–2247.

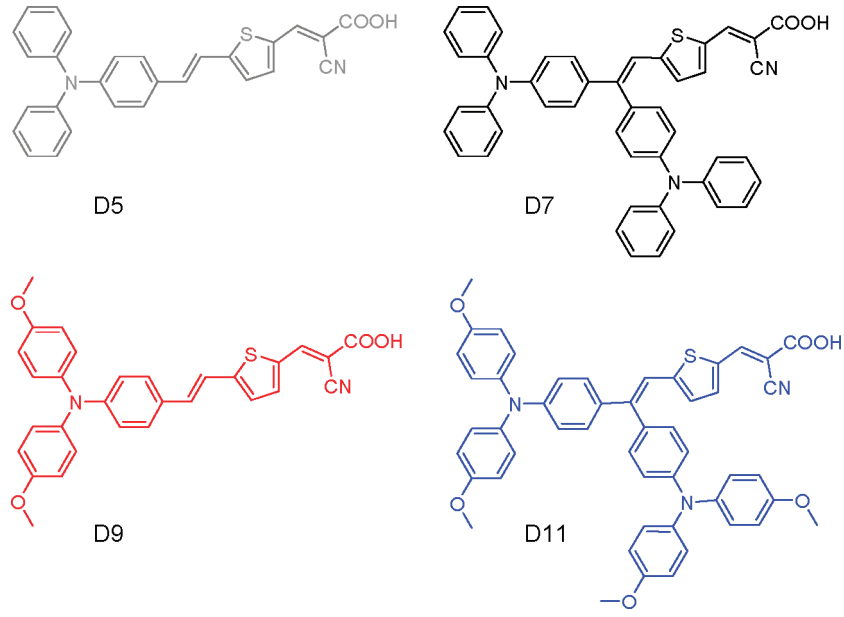

Figure 1. Molecular structures of D5, D7, D9, and D11.

between the lowest unoccupied molecular orbital (LUMO) of the dye and the TiO_2 conduction band. The major factors for low conversion efficiency of many organic dyes in the DSC are the formation of dye aggregates on the semiconductor surface and recombination of conduction-band electrons with triiodide.[17] Therefore, to obtain optimal performance, aggregation of organic dyes and recombination need to be avoided through appropriate structural modification.[18,19] On the basis of this strategy, we have designed and synthesized a series of organic sensitizers, 3-(5-(4-(diphenylamino)styryl)thiophen-2-yl)-2-cyanoacrylic acid (D5),[16] 3-(5-bis(4-(diphenylamino)styryl)thiophen-2-yl)-2-cyanoacrylic acid (D7), 5-(4-(bis(4-methoxyphenylamino)styryl)thiophen-2-yl)-2- cyanoacrylic acid (D9), and 3-(5-bis(4,4′-dimethoxydiphenylamino)styryl)thiophen-2-yl)-2-cyanoacrylic acid (D11). In this paper, we report detailed investigation of photovoltaic performance of the D5, D7, D9, and D11 sensitizers in liquid- and solid-state-based electrolytes.

Results and Discussion

Figure 1 shows the molecular structure of the D5, D7, D9, and D11 organic sensitizers, which were synthesized according to well-known reactions resulting in moderate yields. Aniline was functionalized by an Ullman-type coupling, and the thiophene moiety was coupled to the donor by Wittig reaction (D5 and D9) or Horner−Wadsworth−Emmons reaction (D7 and D11).[20,21] Formylation of the thiophene moiety followed by condensation of the aldehyde by the Knoevenagel protocol in the presence of piperidine yielded the final sensitizers (see Experimental Section for detailed information).

Figure 2 shows the UV/vis spectra of the novel organic sensitizers, D5, D7, D9, and D11, measured in ethanol solution.

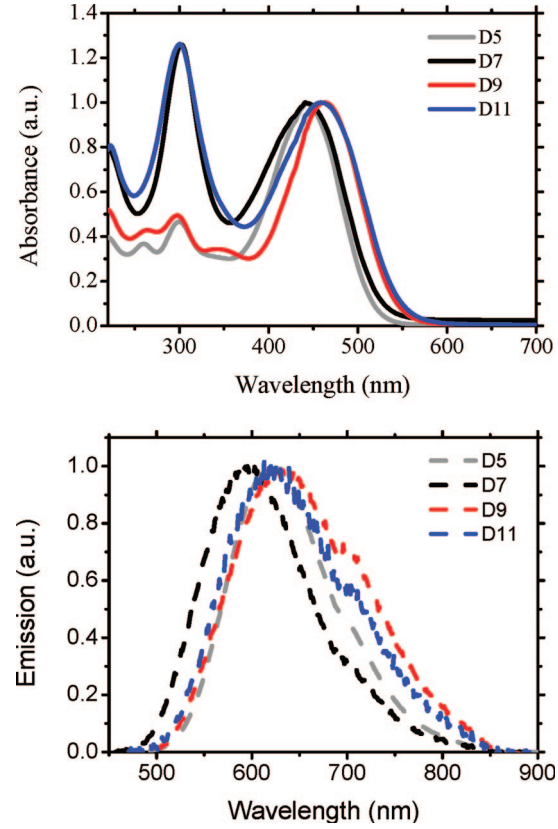

Figure 2. Normalized absorption (solid lines, top) and emission (dashed lines, bottom) spectra of D5 (gray lines), D7 (black lines), D9 (red lines), and D11 (blue lines) measured in ethanol. The emission spectra were obtained by using the same solution by exciting at absorption maximum at 298 K, and the low-energy shoulder is an instrument artifact.

The absorption spectra of the D5 dye displays a strong visible band at 441 nm (ε = 33 000 M^{-1} cm^{-1}) due to the $\pi-\pi^*$ transitions of the conjugated molecule. The D7 sensitizer that contains two diphenylaniline units also exhibits similar spectral properties (absorption maxima at 441 nm, ε = 31 000 M^{-1} cm^{-1}). However, the D9 (462 nm, ε = 33 000 M^{-1} cm^{-1}) and

(17) Liu, D.; Fessenden, R. W.; Hug, G. L.; Kamat, P. V. *J. Phys. Chem. B* **1997**, *101*, 2583–2590.
(18) Burfeindt, B.; Hannappel, T.; Storck, W.; Willig, F. *J. Phys. Chem.* **1996**, *100*, 16463–16465.
(19) Sayama, K.; Tsukagoshi, S.; Hara, K.; Ohga, Y.; Shinpou, A.; Abe, Y.; Suga, S.; Arakawa, H. *J. Phys. Chem. B* **2002**, *106*, 1363–1371.
(20) Wadsworth, W. S., Jr.; Emmons, W. D. *J. Am. Chem. Soc.* **1961**, *83*, 1733–1738.
(21) Hu, Z. Y.; Fort, A.; Barzoukas, M.; Jen, A. K. Y.; Barlow, S.; Marder, S. R. *J. Phys. Chem. B* **2004**, *108*, 8626–8630.

Table 1. Experimental Spectral and Electrochemical Properties of the Dyes

dye	Abs_{max}[a] [nm]	ε [$M^{-1}cm^{-1}$]	Em_{max}[a] [nm]	$E_{(S+/S)}$[b] [V] vs NHE	$E_{(0-0)}$[c] [V] (Abs/Em)	$E_{(S+/S^*)}$[d] [V] vs NHE
D5	441	33 000	621	1.08	2.37	−1.29
D7	441	31 000	595	1.07	2.42	−1.35
D9	462	33 000	632	0.91	2.32	−1.41
D11	458	38 000	620	0.92	2.33	−1.41

[a] Absorption and emission spectra of dyes in ethanol solution. [b] The ground-state oxidation potential of the dyes was measured with DPV under the following conditions: Pt working electrode and Pt counter electrode; electrolyte, 0.1 M tetrabutylammonium hexafluorophosphate, $TBA(PF_6)$, in acetonitrile. Potentials measured vs Fc^+/Fc were converted to normal hydrogen electrode (NHE) by addition of +0.63 V. [c] 0−0 transition energy, $E_{(0-0)}$, estimated from the intercept of the normalized absorption and emission spectra in ethanol. [d] Estimated LUMO energies, $E_{(LUMO)}$, vs NHE from the estimated highest occupied molecular orbital (HOMO) energies obtained from the ground-state oxidation potential by adding the 0−0 transition energy, $E_{(0-0)}$.

D11 (458 nm, $\varepsilon = 38\,000\ M^{-1}\ cm^{-1}$), which contain methoxy groups, show red-shifted absorption maxima compared to the D5 and D7 sensitizers (see Table 1). The absorption spectra of D5, D7, D9, and D11 adsorbed onto 3.5 μm thick TiO_2 electrodes are similar to the corresponding solution spectra but exhibit a small red shift due to the interaction of the anchoring groups with the surface titanium ions.

The DPV of D5 sensitizer measured in acetonitrile containing 0.1 M $TBA(PF_6)$ with 0.1 V scan rate shows a symmetrical peak at 1.07 V vs NHE because of the oxidation of the 4-(diphenylamino) group. It is interesting to note that in D9 sensitizer, the oxidation potential (0.91 V vs NHE) shifted cathodically by 0.11 V, compared to that in the D5 sensitizer, demonstrating the extent of destabilization of HOMO caused by dimethoxy groups. The difference in the oxidation potential between D7 and D11 sensitizers is consistent with that of D5 and D9 sensitizers. The destabilization of the HOMO of the D9 and D11 sensitizers caused by methoxy substitution is reflected in absorption spectra of these sensitizers.

The excited-state oxidation potential of the sensitizer plays an important role in the electron-injection process. By neglecting any entropy change during light absorption, the value can be derived from the ground-state oxidation couple and the 0−0 excitation energy, $E_{(0-0)}$, according to eq 1.

$$E(S^+/S^*) = E(S^+/S) - E_{(0-0)} \quad (1)$$

From the absorption/emission spectra, $E_{(0-0)}$ energies of 2.37, 2.42, 2.32, and 2.33 eV were extracted for D5, D7, D9, and D11, respectively. The excited-state oxidation potential of these sensitizers is more negative (−1.29 V vs NHE) than the equivalent potential for N719 sensitizer (− 0.98 V vs NHE) and the TiO_2 conduction band.[13] Therefore, these types of sensitizers have sufficient driving force for electron injection to TiO_2 and become very attractive for other semiconductor materials having conduction bands more negative than the conduction bands of TiO_2. An increased gap between the conduction band and the redox couple yields higher open-circuit voltage, enhancing the cell efficiency considerably. On the other hand, the oxidation potential of the sensitizers is more positive than the I^-/I_3^- redox couple (~0.4 V vs NHE), ensuring that there is enough driving force for the dye regeneration reaction to compete efficiently with the recapture of the injected electrons by the dye cation radical.

To gain insight into the geometrical and electronic structure of the new dyes, we performed density functional theory (DFT) calculations on the three organic sensitizers by using the Gaussian03 program package.[22] In particular, we used B3LYP as exchange-correlation functional[23] and 6-31g* as basis set.[24] Solvation effects were included by means of the Polarizable Continuum model.[24] The geometrical structures of the dyes have been optimized in vacuo, and time-dependent (TD) DFT excited-state calculations were performed in water solution. Solvation effects were included by means of the Polarizable Continuum model.[25]

We report in Figure 3 the calculated molecular orbital energy diagram for D5, D9, and D11, along with isodensity plots of the HOMO and LUMO for the D9 and D11 systems (the HOMO and LUMO for D5, not shown, have localization similar to that in D9).[16] The D9 HOMO is a π orbital delocalized throughout the entire molecule, whereas in D11, the almost degenerate HOMO and HOMO-1 (not shown) couple, although having a similar character, is mainly localized on the two methoxy-substituted diphenylamino moieties and on the double C−C bond, with little contributions from the thiophenes and cyanoacrylic acid groups. The LUMO is, on the other hand, very similar in D5, D9, and D11, being in all cases a single π^* orbital delocalized across the thiophenes and cyanoacrylic acid groups, with sizable contributions from the latter. Given LUMO composition, its energy is less sensitive than that of the HOMO to methoxy substituents. The cyanoacrylic acid contribution to the LUMO, which represents the final state in the charge-transfer transitions characterizing the new dyes, see below, is relevant to ensure a high electronic coupling between the dye excited state and the TiO_2 conduction band, which in turn, translates into high photocurrent densities in DSC devices. The electronic structures of the novel organic sensitizers are quite similar to those of the recently reported 3-{5-[*N*,*N*-bis(9,9-dimethylfluorene-2-yl)phenyl]-thiophen-2-yl}−2-cyano-acrylic acid (JK-1) and 3-{5′-[*N*,*N*-bis(9,9-dimethylfluorene-2-yl)phenyl]-2,2′-bisthiophen-5-yl}−2-cyano-acrylic acid (JK-2) dyes,[15] with the HOMO (and HOMO-1 for D11) and LUMO being the only molecular orbitals present in the energy range exceeding 1 eV. For D5, D9, and D11, we calculate the lowest singlet−singlet excitation energy at 2.03, 1.88, and 1.73 eV, respectively. For D5 and D9, the lowest transition corresponds to a single HOMO → LUMO excitation and is followed in D9 by a HOMO-1 → LUMO transition at 2.83 eV. For D11, the lowest excitation is followed at 1.89 eV by an almost degenerate transition; both excited states are originated by HOMO → LUMO and HOMO-1 → LUMO contributions, showing therefore a strong charge-transfer character. The two almost degenerate lowest excitations of D11 are followed, at higher energy, by a HOMO-2 → LUMO transition at 2.82 eV, therefore with similar energy and character as in D9.

It is worth comparing our calculated electronic structure to the available electrochemical and spectroscopic data obtained in the context of the present investigation. The electrochemical oxidation potential data are consistent with the trends in the HOMOs and LUMOs energies calculated for D5, D9, and D11, showing a slight increase (by 160 mV) in the oxidation potential when going from D5 to D9 and no appreciable variations of

(22) Frisch, M. J. et al. *Gaussian 03*, revision B.05; Gaussian, Inc.: Wallingford, CT, 2004.
(23) Becke, A. D. *J. Chem. Phys.* **1993**, *98*, 5648–5652.
(24) Ditchfield, R.; Herhe, W. J.; Pople, J. A. *J. Chem. Phys.* **1971**, *54*, 724–728.
(25) (a) Barone, V.; Cossi, M. *J. Phys Chem. A* **1998**, *102*, 1995–2001. (b) Cossi, M.; Rega, N.; Scalmani, G.; Barone, V. *J. Comput. Chem.* **2003**, *24*, 669–681.

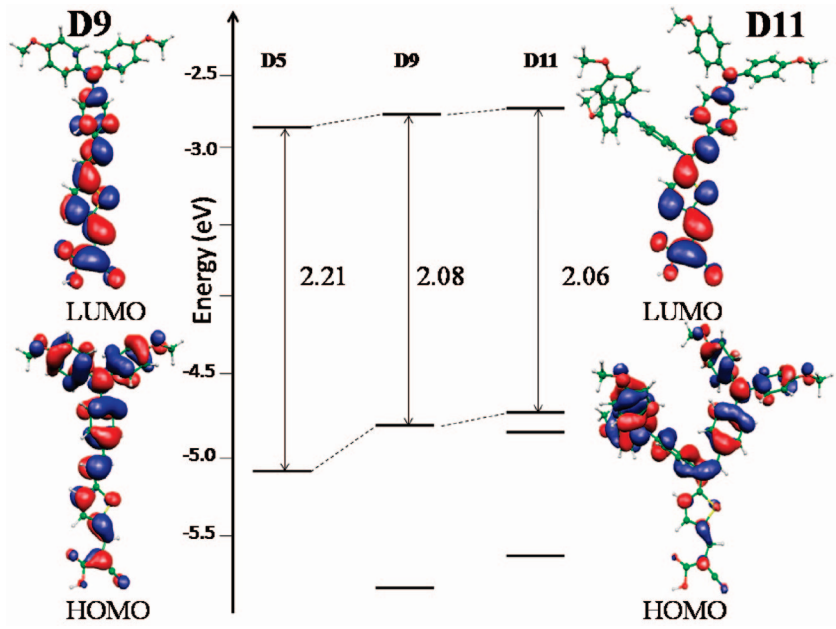

Figure 3. Molecular orbital energy diagram and isodensity surface plots of the HOMO and LUMO of D9 and D11.

this parameter when going from D9 to D11. The decreased oxidation potential measured for D9 compared to that of D5 is directly related to the calculated HOMO destabilization (0.18 eV), related to the presence of the electron-donating methoxy-substituents. The lowest TDDFT excitation energies, although qualitatively reproducing the similar spectroscopic behavior of D9 and D11 with absorption maxima at ca. 2.7 eV, considerably underestimate both the absorption maxima and the estimated $E_{(0-0)}$ transitions, which are determined at ca. 2.3 eV for both dyes. This underestimate of the lowest excitation energies, which shows up also in terms of HOMO−LUMO gaps, see Figure 3, was already found in similar charge-transfer JK-1 and JK-2 dyes[15] and can be related to a deficiency of DFT to deal with extensively delocalized states, such as those we are facing in the present cases.

The D5, D7, D9, and D11 sensitizers have been used to manufacture solar cell devices to explore current−voltage characteristics by using 7 (transparent) + 5 (scattering) μm TiO_2 layers. Figure 4 shows the incident monochromatic photon-to-current conversion efficiency (IPCE) obtained with a sandwich cell by using 0.6 M *N*-methyl-*N*-butyl imidazolium iodide, 0.04 M iodine, 0.025 M LiI, 0.05 M guanidinium thiocyanate, and 0.28 M *tert*-butylpyridine in 15/85 (v/v) mixture of valeronitrile and acetonitrile as redox electrolyte. The IPCE data of all sensitizers plotted as a function of excitation wavelength exhibit a high plateau at 85%. D7 showed IPCE to be blue-shifted around 10 nm, which is coincident with the result of absorption spectra, as mentioned above. The IPCE spectra of the D9 and D11 sensitizers that contain methoxy groups exhibit 30 nm red shift compared to the D5 and D7 sensitizers, which is consistent with the absorption spectra. Under standard global AM 1.5 solar conditions, the D5-sensitized cell gave a short-circuit photocurrent density (J_{sc}) of 12.0 ± 0.20 mA/cm^2, an open-circuit voltage (V_{oc}) of 688 ± 10 mV, and a fill factor (*ff*) of 0.72 ± 0.02, corresponding to an overall conversion efficiency η, derived from the equation $\eta = J_{sc}V_{oc}ff$/light intensity, of 5.94% (see Table 2). The D7-sensitized cell gave J_{sc} of 11.00 ± 0.20 mA/cm^2, V_{oc} of 695 ± 10 mV, and *ff* of 0.71 ± 0.02, corresponding to an overall conversion efficiency η of 5.43%.

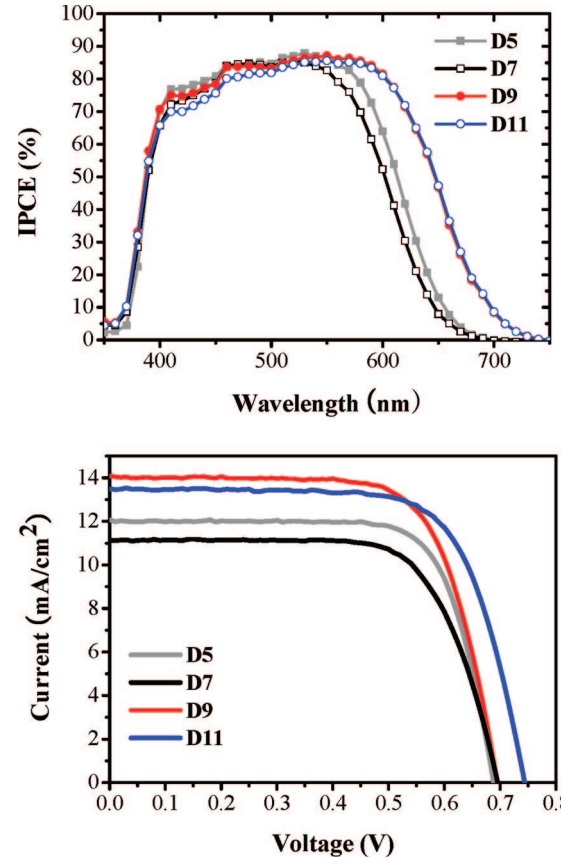

Figure 4. IPCE (top) and current−voltage characteristics (bottom) obtained with a nanocrystalline TiO_2 film supported on FTO conducting glass and derivatized with monolayer of D5 (gray line), D7 (black line), D9 (red line), and D11 (blue line).

The reason for the low efficiency of D7-sensitized cell compared to the D5 cell is the lower photocurrent due to the narrow IPCE spectra of D7 compared those of D5. In contrast, D9- and D11-sensitized cells exhibited higher photovoltaic performance when compared to D5-sensitized cells because of enhanced spectral

Table 2. Current−Voltage Characteristics Obtained with a TiO_2 Film (7 + 5 μm) on FTO Conducting Glass and Derivatized with Monolayer of D5, D7, D9, and D11

dye	J_{sc} (mA/cm^2)	V_{oc} (mV)	*ff*	η (%)
D5	12.00	688	0.72	5.94
D7	11.00	695	0.71	5.43
D9	14.00	694	0.71	6.90
D11	13.50	744	0.70	7.03

Table 3. Current−Voltage Characteristics Obtained with D11-Sensitized Solar Cells for Various Thicknesses of the Nanocrystalline TiO_2 Films

thickness (μm)	J_{sc} (mA/cm^2)	V_{oc} (mV)	*ff*	η (%)
2.5 + 5	12.30	765	0.70	6.59
5 + 5	12.90	753	0.70	6.80
7 + 5	13.50	744	0.70	7.03
10 + 5	13.90	744	0.70	7.23

response. The D9-sensitized cell yielded J_{sc} of 14.00 ± 0.20 mA/cm^2, V_{oc} of 694 ± 10 mV, and *ff* of 0.71 ± 0.02, corresponding to an overall conversion efficiency η of 6.90%. And the D11-sensitized cell (having four methoxy groups) yielded J_{sc} of 13.90 ± 0.20 mA/cm^2, V_{oc} of 744 ± 10 mV, and *ff* of 0.70 ± 0.02, corresponding to an overall conversion efficiency η of 7.23%. The higher efficiency of the D9 and D11 sensitizers compared to the D5 and D7 sensitizers demonstrates the beneficial influence of alkoxy units on photovoltage and photocurrent, caused by the enhanced red response. The increased photovoltage of D11-sensitized solar cell (~50mV, see Table 2) compared to that of the D5-sensitized solar cell is mainly due to the increased lifetime of the conduction-band electrons; a detailed discussion about this effect will be done in the section on electron kinetics.

In order to see the impact of the high molar extinction coefficient of these sensitizers on photovoltaic properties, we have fabricated solar cells having TiO_2 films of various thicknesses and using D11 sensitizer. The photocurrent increased with the thickness of TiO_2 nanocrystalline layer; on the other hand, the photovoltage decreased with increasing thickness (see Table 3). The increased surface area due to higher thickness of TiO_2 film allows for better light harvesting, which however enhances the possibility for injected electrons to recombine with the oxidized redox species triiodide. The devices using a 2.5 μm thin TiO_2 layer yielded remarkably high photocurrent (12.3 mA/cm^2) and 79% IPCE, which we have attributed to the high molar extinction coefficient of the dye.

The V_{oc} of a DSC is determined by the difference between the quasi-Fermi level ($_nE_F$) in the TiO_2 under illumination and the Fermi level of the electrolyte (redox potential, $E_{F,redox}$). The increase in V_{oc} could be caused by two different mechanisms: one is a retardation of the recombination between injected electrons and oxidized species in the electrolyte, and another is a band edge movement with respect to the redox potential.[26,27] The electron lifetime in a DSC can be estimated from the photovoltage response to a small perturbing light pulse.[27] The apparent photovoltage decay at the open-circuit condition can be obtained from fitting the following exponential equation:

$$\Delta V_{photo}(t) = \Delta V_{photo}(0)\exp(-t/\tau) \qquad (2)$$

where t is the time at the end of a small light pulse, and τ is the apparent electron lifetime. The apparent electron lifetime can be obtained from fitting the photovoltage decay with an exponential function. Figure 5 shows a plot for the change in

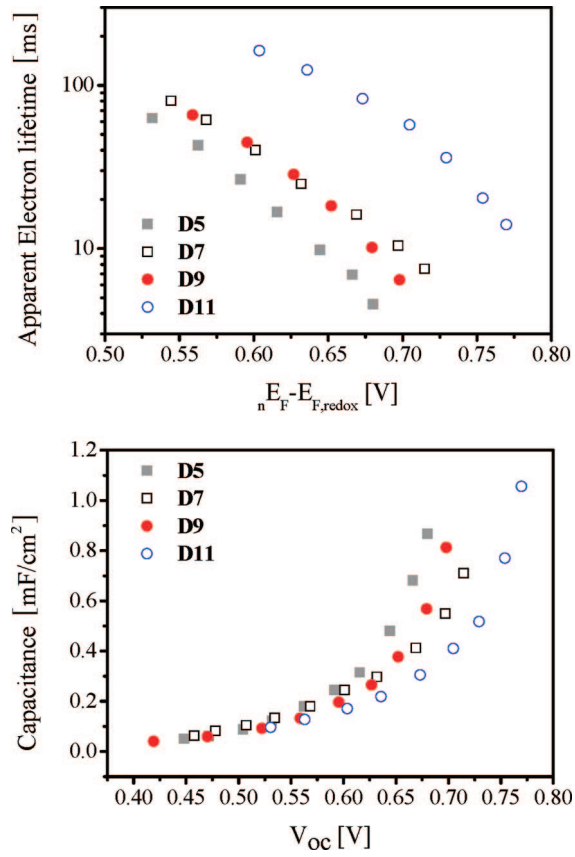

Figure 5. Electron lifetime (top) and capacitance (bottom) obtained with a 7 μm transparent nanocrystalline TiO_2 film supported onto a conducting glass sheet and derivatized with a monolayer of D5 (gray), D7 (black), D9 (red), and D11 (blue).

electron lifetime (τ) for the above-discussed DSCs based on 7 μm transparent TiO_2 films as a function of V_{oc} ($_nE_F - E_{F,redox}$), resulting from various bias-light intensities. The apparent electron lifetimes (τ) in D7- and D11-sensitized solar cell are ~2.0 and ~7.5 times longer than that of the solar cell sensitized with the D5, which shows the effect of disubstituted donor moieties on the electron lifetime. The disubstituted donor moieties in D7 and D11 prevent the triiodide in the electrolyte from recombining with injected electrons in the TiO_2 condution band, leading to increased open-circuit potentials when compared to the D5 sensitizer. The long apparent electron lifetimes (τ) in D9- and D11-sensitized solar cell when compared to that of D5-sensitized solar cell are plausibly caused by the effect of methoxy moieties. D11-sensitized solar cell consequently showed the longest electron lifetime, which is presumably caused by the synergetic effect of disubstituted donor moieties and methoxy moieties. Figure 5 (bottom) shows the chemical capacitance as a function of V_{oc} at different light intensities. The chemical capacitance follows a characteristic exponential rise with increasing forward bias. The low chemical capacitance at fixed V_{oc} might be due to either a negative shift of the conduction band or a longer lifetime of electrons. The electron lifetimes of D7-, D9-, and D11-sensitized solar cells were longer than that of D5, as mentioned above, and thus contributed to lowering the chemical capacitance. Consequently, the D11-

(26) Zhang, Z.; Evans, N.; Zakeeruddin, S. M.; Humphry-Baker, R.; Grätzel, M. *J. Phys. Chem. C* **2007**, *111*, 398.
(27) Schlichthörl, G.; Huang, S. Y.; Sprague, J.; Frank, A. J. *J. Phys. Chem. B* **1997**, *101*, 8141–8155.

Table 4. Current−Voltage Characteristics Obtained with D5-, D7-, D9-, and D11-Sensitized Solar Cells as Solid-State Cells[a]

dye	J_{sc} (mA/cm^2)	V_{oc} (mV)	*ff*	η (%)
D5	6.31	865	0.57	3.11
D7	5.02	785	0.71	2.79
D9	7.72	756	0.56	3.25
D11	5.85	811	0.63	3.01

[a] The solid-state cell configuration was used to measure this spectrum. The 1.7 μm TiO_2 film composed of 20 nm anatase particles was used for derivation of sensitizers, and the Spiro was incorporated as a hole conductor under evaporated gold cathode.

sensitized solar cell gives the highest V_{oc} because of both disubstituted donor and methoxy groups.

These organic dyes were evaluated as sensitizers for the solid-state dye-sensitized solar cells in which spiro-MeOTAD hole conductor is used as a redox couple.[28,29] Under standard global AM 1.5 solar conditions, all the D-series dye-sensitized cells showed only 50% of their liquid-electrolyte counterparts in overall efficiency. D9 gave the best performance, J_{sc} of 7.72 mA/cm^2, V_{oc} of 756 mV, and *ff* of 0.56, leading to an overall conversion efficiency η of 3.25% (see Table 4). The D9-sensitized cell demonstrated an almost linear behavior under different light intensities, ranging from 9.2 to 99% sun with a slightly higher efficiency (~3.5%) at low intensity (Figure 6, top panel). The IPCE of the D9-sensitized device exhibited relatively high values of 40−50% in the range of 420−530 nm (Figure 6b), which are higher than that of the standard N719-based cell.[29] Considering the film thickness (1.7 μm) of TiO_2 used, the results from D-series sensitizers look promising in the application of solid-state cells.

We note that in a solid-state device, the dyes with one diphenylaniline moiety (D5 and D9) always gave a higher efficiency than the dyes that contain two diphenylaniline groups (D7 and D11). Also, the dyes that contain methoxy-donor groups (D9 and D11) showed a better photovoltaic performance compared to the corresponding sensitizers (D5 and D7) that contain no methoxy group. Those observations in solid-state cells are somewhat different from the results in liquid cells, which means that other factors, such as hole-transfer yield and pore penetration by intimate contacts between dye and hole conductor, should also be considered in the performance of solid-state cells, as pointed out recently.[28c] The solid-state solar cell with the D9 sensitizer exhibited best performance, which can be ranked to the second place next to indoline dye (D102), which showed an efficiency of 4.1% (J_{sc} of 7.7 mA/cm^2, V_{oc} of 866 mV, and *ff* of 0.61).[29] It is remarkable to note that the D9 dye has a lower extinction coefficient (ϵ = 33 000 M^{-1} cm^{-1}) compared to that of the D102 sensitizer (ϵ = 55 800 M^{-1} cm^{-1} at 491 nm); yet, the photocurrent of both sensitizers is ~7.7 mA/cm^2. These data indicate that the D9 sensitizer has a better absorbed photon-to-current conversion efficiency than D102 for the same device structure of solid-state cell.

The D5-, D7-, and D9-sensitized solar cells were subjected to accelerated testing in a solar simulator at 100 mW cm^{-2} intensity at 60 °C. The cells showed reasonable photochemical and thermal stability, and the efficiency remained 70% of the initial value after 1000 h. However, under similar conditions, the D11-sensitized solar cells interestingly showed excellent photochemical and thermal stability, and the efficiency remained 90% of the initial value after 1000 h.

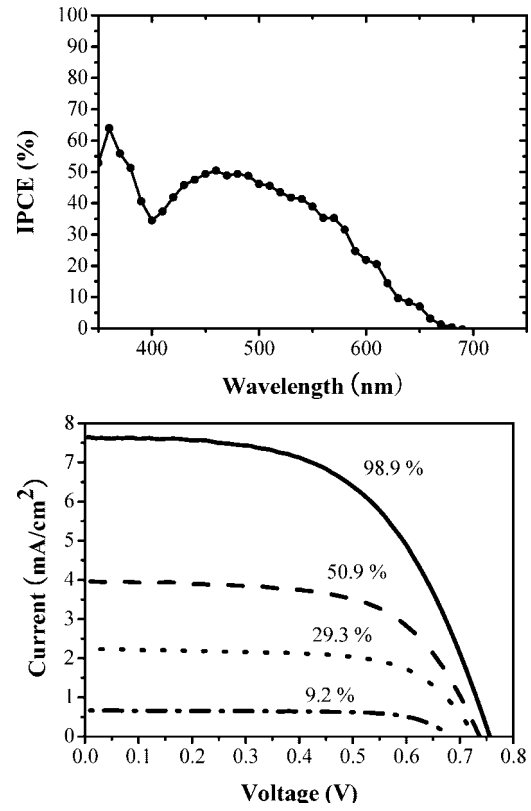

Figure 6. IPCE (top) and current−voltage characteristics (bottom) obtained with solid-state solar cells derivatized with D9.

Conclusion

In summary, we have developed a series of organic sensitizers, which demonstrate the effect of substituted donor groups on controlling optical and photovoltaic properties. The electron kinetics data of the DSCs, with the D5, D7, D9, and D11 organic dyes, together with DFT/TDDFT calculations, unravel the substitution effect, which prevents triiodide present in the electrolyte from recombining with injected electrons in the TiO_2, leading to increased open-circuit potentials. For thin-film solid-state solar cells based on these organic dyes, D9 showed an excellent performance. Structural modification of D9 to increase the molar extinction coefficient is anticipated to give even better performance.

Experimental Section

Materials and Measurements. The UV/visible and emission spectra of the dyes in solution were recorded on a Cary Varian spectrophotometer and a HR-2000 Ocean Optics fiber optics spectrophotometer, respectively.

Differential pulse voltammetry was performed with a CH Instruments 660 potentiostat by using 0.1 M TBA(PF_6) in acetonitrile (Fluka, >99.9%) as supporting electrolyte. A Pt working electrode, a Pt counter electrode, and an Ag/Ag$^+$ reference electrode were used. The system was internally calibrated with ferrocene/ferrocenium (Fc/Fc$^+$).

For photovoltaic measurements of the DSCs, the irradiation source was a 450 W xenon light source (Osram XBO 450, U.S.A.)

(28) (a) Snaith, H. J.; Schmidt-Mende, L.; Grätzel, M. *Phys. Rev. B* **2006**, *74*, 045306. (b) Snaith, H. J.; Grätzel, M. *Appl. Phys. Lett.* **2006**, *89*, 262114. (c) Kroeze, J. E.; Hirata, N.; Schmidt-Mende, L.; Orizu, C.; Ogier, S. D.; Carr, K.; Grätzel, M.; Durrant, J. R. *Adv. Func. Mater.* **2006**, *16*, 1832–1838.

(29) Schmidt-Mende, L.; Bach, U.; Humphry-Baker, R.; Horiuchi, T.; Miura, H.; Ito, S.; Uchida, S.; Grätzel, M. *Adv. Mater.* **2005**, *17*, 813–815.

using a Tempax 113 solar filter. The output power of the AM 1.5 solar simulator was calibrated by using a reference Si photodiode equipped with a colored matched IR-cutoff filter (KG-3, Schott) in order to reduce the mismatch in the region of 350−750 nm between the simulated light and AM 1.5 to less than 2%.[30] The measurement delay of photo $I-V$ characteristics of DSCs was fixed to 40 ms. The measurement of IPCE was plotted as a function of excitation wavelength by using the incident light from a 300 W xenon lamp (ILC Technology, U.S.A.), which was focused through a Gemini-180 double monochromator (Jobin Yvon Ltd., U.K.). The photoelectrochemical measurements were carried out by using a Xe lamp source designed to give 100 mW/cm^2 at AM 1.5 G sun light and a voltage source meter to sweep the voltage across the irradiated cell and, at the same time, measure the generated current. The IPCE is determined by wavelength scanning the light source on the cell and measuring the short-circuit current as a function of wavelength. Photo-generated transients were observed by using an exciting pulse generated by green-light-emitting (535 nm) diodes with a white-light bias. From the current decay, the photo-generated charge in the cell is measured. The corresponding voltage decay gives the electron lifetime.

Dye-Sensitized Solar Cells. The photo-anodes composed of nanocrystalline TiO_2 were prepared by using a previously reported procedure.[30,31] FTO glass plates (Nippon Sheet Glass, Solar 4 mm thickness) were used for transparent conducting electrodes. After $TiCl_4$ treatment, a paste composed of 20 nm anatase TiO_2 particles for the transparent nanocrystalline layer was coated on the FTO glass plates by screen printing. This coating−drying procedure was repeated to increase the thickness to the required value. After drying the nanocrystalline TiO_2 layer, a paste for the scattering layer containing 400 nm sized anatase particles (CCIC, HPW-400) was deposited by two screen printings. The resulting layer was composed of various thicknesses of transparent layer and 5 μm of scattering layer, the thicknesses being measured by using Alpha-step 200 surface profilometer (Tencor Instruments, San Jose, CA). The TiO_2 electrodes were gradually heated under an air flow, and then, the TiO_2 electrodes were treated by $TiCl_4$ and sintered at 500 °C for 30 min. The TiO_2 electrodes were immersed into the D5, D7, D9, and D11 solutions (0.3 mM in ethanol containing 10 mM 3a,7a-dihydroxy-5b-cholic acid (Cheno)) and kept at room temperature for 4 h. Counter electrodes were prepared by coating with a drop of H_2PtCl_6 solution (2 mg of Pt in 1 mL of ethanol) on a FTO plate (TEC 15/2.2 mm thickness, Libbey-Owens-Ford Industries) and heating at 400 °C for 15 min. The dye-adsorbed TiO_2 electrode and Pt counter electrode were assembled into a sealed sandwich-type cell by heating with a hot-melt ionomer film (Surlyn 1702, 25 μm thickness, Du-Pont) as a spacer between the electrodes. An electrolyte solution (electrolyte of 0.6 M *N*-methyl-*N*-butyl imidiazolium iodide, 0.04 M iodine, 0.025 M LiI, 0.05 M guanidinium thiocyanate, and 0.28 M *tert*-butylpyridine in 15/85 (v/v) mixture of valeronitrile and acetonitrile) was used as redox couple. Finally, the hole was sealed by using additional Bynel and a cover glass (0.1 mm thickness). An antireflection and UV cut-off film ($\lambda <$ 380 nm, ARKTOP, Asahi Glass) was attached to the DSC surface. In order to reduce scattered light from the edge of the glass electrodes of the dyed TiO_2 layer, light shading masks were used on the DSCs, so that the active area of DSCs was fixed to 0.2 cm^2.

For solid-state solar cells, ~100 nm compact layer of TiO_2 was deposited by spray pyrolysis after cleaning FTO glass substrates (15Ω/, Pilkington) with Helmanex (a detergent), acetone, and ethanol. A nanoporous layer (~1.7 μm) of 20 nm TiO_2 was prepared by doctor-blading technique, followed by heating slowly to 500 °C; then, the preparation was baked at this temperature for 30 min under an oxygen flow. After cooling, the as-prepared films were treated with 0.02 M $TiCl_4$ aqueous solution overnight, then washed with a copious amount of deionized water, and dried. Prior to the dye uptake, the substrates were annealed at 500 °C for 30 min under oxygen flow and then cooled to ~80 °C before being put into the dye solutions for 6 h. After soaking in the dye solution, the substrates were rinsed in acetonitrile, and the hole-conducting matrix was spin-coated on their upper surface by following our typical procedures.[28] The hole-transporting material used was 2,2′,7,7′-tetrakis(*N*,*N*-dimethoxyphenyl-amine)-9,9′-spirobifluorene (spiro-MeOTAD), which was dissolved in chlorobenzene. *tert*-Butyl pyridine and Li[CF_3SO_2]$_2$N were added as additives. The device fabrication was finished by evaporating a 50 nm gold electrode on the top.

Synthesis of Sensitizers. All reactions were carried out under nitrogen atmosphere with the use of standard inert atmosphere and Schlenk techniques. Dichloromethane (DCM), dimethylformamide (DMF), hexane, and tetrahydrofuran (THF) were dried by passing through a solvent column composed of activated alumina. ^{1}H and ^{13}C NMR spectra were recorded on Bruker 500 and 400 MHz instruments by using the residual signals δ 7.26 and 77.0 ppm from $CDCl_3$, 2.50 and 39.4 ppm from d_6-DMSO, and 2.05, 29.84, and 206.26 ppm from d_6-acetone as internal references for ^{1}H and ^{13}C, respectively. HR-MS was performed by using a Q-Tof Micro (Micromass Inc., Manchester, England) mass spectrometer equipped with Z-spray ionization source.

3-(5-(4-(Diphenylamino)styryl)thiophen-2-yl)-2-cyanoacrylic Acid (D5). The synthetic procedure and characterizations were presented in an earlier publication. [16]

3-(5-Bis(4-(diphenylamino)styryl)thiophen-2-yl). To a stirred solution of 4,4′-bis(*N*,*N*-diphenylamino)benzophenone[32] (1.84 g, 3.65 mmol) and DMF (50 mL), t-BuOK (1.02 g, 9.13 mmol) was added, and the mixture was cooled to 0 °C over 30 min. Diethyl thiophenephosphonate (851 mg, 3.64 mmol) in DMF (10 mL) was added dropwise, and the solution was kept at 0 °C for 1 h. The reaction mixture was allowed to warm to ambient temperature and was stirred under nitrogen atmosphere for 24 h. Ether/water extraction, followed by solvent evaporation and column chromatography over silica gel (20% DCM in petroleum ether) yielded a yellow oil (1.3 g, 61%). ^{1}H NMR (500 MHz, d_6-acetone): δ 7.40 (s, 1H), 7.32 (m, 10H), 7.25 (d, J = 5.1 Hz, 1H), 7.17 (m, 8H), 7.07 (m, 9H), 6.97 (d, J = 8.8 Hz, 2H), 6.93 (d, J = 3.6 Hz, 1H). ^{13}C NMR (125 MHz, d_6-acetone): 149.7, 149.6, 149.5, 149.1, 143.5, 140.6, 137.6, 135.3, 133.1, 131.3, 130.9, 129.3, 128.2, 127.9, 126.3, 126.3, 126.2, 125.1, 124.9, 124.7, 121.7. MS (APCI-ES) *m*/*z*: 597.3 $[M + H]^+$.

3-(5-Bis(4-(diphenylamino)styryl)thiophen-2-yl)-2-carbaldehyde. 3-(5-bis(4-(diphenylamino)styryl)thiophen-2-yl) (1.3 g, 2.23mmol) was dissolved in DMF and cooled to −78 °C. The mixture was kept under nitrogen atmosphere. To the mixture, $POCl_3$ (0.34 g, 2.23 mmol) was added dropwise. The reaction mixture was allowed to warm to 0 °C, whereupon it turned red. The mixture was heated to 50 °C for 3 h. The reaction mixture was cooled to ambient temperature and quenched by aq HCl (0.1 M, 100 mL). The solution was washed with brine/ether. The organic phase was dried with $NaSO_4$. The solvent removal, followed by column chromatography (10% petroleum ether in DCM), yielded the product as an orange solid (0.86 g, 63%), mp 234.0−234.8. ^{1}H NMR (500 MHz, d_6-acetone): δ 9.85 (s, 1H), 7.75 (d, J = 3.9 Hz, 1H), 7.51 (s, 1H), 7.41 (d, J = 8.9 Hz, 2H), 7.34 (m, 8H), 7.27 (d, J = 4.0 Hz, 1H), 7.22 (m, 6H), 7.17 (d, J = 8.6 Hz, 2H), 7.09 (m, 8H), 6.99 (d, J = 8.8 Hz, 2H). ^{13}C NMR (125 MHz, d_6-acetone): 184.8, 152.7, 150.6, 149.7, 149.2, 145.9, 144.9, 138.0, 132.8, 131.9, 131.4, 129.8, 127.3, 126.7, 126.2, 125.5, 124.9, 124.0, 120.9. MS (APCI-ES) *m*/*z*: 625.3 $[M + H]^+$.

3-(5-Bis(4-(diphenylamino)styryl)thiophen-2-yl)-2-cyanoacrylic Acid (D7). A 30 mL acetonitrile solution of 3-(5-bis(4-(diphenylamino)styryl)thiophen-2-yl)-2-carbaldehyde (404 mg, 0.07

(30) Wang, P.; Zakeeruddin, S. M.; Comte, P.; Charvet, R.; Humphry-Baker, R.; Grätzel, M. *J. Phys. Chem. B* **2003**, *107*, 14336–14341.
(31) Nazeeruddin, M. K.; Péchy, P.; Renouard, T.; Zakeeruddin, S. M.; Humphry-Baker, R.; Comte, P.; Liska, P.; Le, C.; Costa, E.; Shklover, V.; Spiccia, L.; Deacon, G. B.; Bignozzi, C. A.; Grätzel, M. *J. Am. Chem. Soc.* **2001**, *123*, 1613–1624.
(32) Plater, M. J.; Jackson, T. *Tetrahedron* **2003**, *59*, 4673–4685.

mmol), cyanoacetic acid (56 mg, 0.07 mmol), and piperidine (1.7 mg, 0.02 mmol) was refluxed for 4 h under nitrogen atmosphere. Purification by extraction (petroleum ether and aq HCl (0.1 M)) and filtration of the formed solid yielded the product as a dark red solid, D7 (254 mg, 56%), mp 214.5−215.5 °C. ^{1}H NMR (500 MHz, d_6-DMSO): δ 8.29 (s, 1H), 7.80 (d, J = 4.1 Hz, 1H), 7.49 (s, 1H), 7.30 (m, 11H), 7.19 (d, J = 7.6 Hz, 4H), 7.06 (m, 12H), 6.90 (d, J = 8.8 Hz, 2H). ^{13}C NMR (125 MHz, d_6-DMSO): 163.8, 151.2, 147.9, 147.5, 146.9, 146.5, 146.3, 143.8, 139.3, 135.0, 133.9, 130.6, 130.5, 129.6, 129.5, 128.1, 124.9, 124.5, 123.6, 123.5, 122.5, 121.7, 118.7, 116.4, 96.8. HR-MS (TOF MS ESI) *m/z*: 714.2186 [M + Na^+]. Calcd for $C_{23}H_{17}NNaOS$ (M + Na^+): 714.2191.

Bis-(4-methoxyphenyl)-phenyl-amine. A mixture of aniline (1.02 g, 10.4 mmol), copper powder (4.55 g, 72 mmol), K_2CO_3 (18.56 g, 134 mmol), 18-crown-6 (100 mg), and iodoanisol (29.43 g, 126 mmol) was heated to reflux at 188 °C under nitrogen atmosphere with stirring for 30 h. The reaction mixture was allowed to cool to ambient temperature and was dissolved in DCM. The solution was washed with distilled water, and the organic phase was dried with $NaSO_4$ and concentrated by evaporation. Column chromatography (10% DCM in petroleum ether) yielded the product as a light yellow solid (2.19 g, 68%). ^{1}H NMR (500 MHz, $CDCl_3$): δ 7.20−7.15 (m, 2H), 7.06 (d, J = 8.91 Hz, 4H), 6.95 (d, J = 7.82 Hz, 2H), 6.87 (t, J = 7.28, 7.28 Hz, 1H), 6.83 (d, J = 8.98 Hz, 4H), 3.80 (s, 6H). ^{13}C NMR (125 MHz, d_6-acetone): 155.7, 148.8, 141.2, 128.9, 126.4, 120.9, 120.6, 114.6, 55.5. MS (APCI-ES) *m/z*: 306.1 [M + H]$^+$.

5-(4-(Bis(4-methoxyphenylamino)styryl)thiophen-2-yl)-2-carbaldehyde.[33] This compound was synthesized from bis-(4-methoxyphenyl)-phenyl-amine following the reported procedure.[33]

5-(4-(Bis(4-methoxyphenylamino)styryl)thiophen-2-yl)-2-cyanoacrylic Acid (D9). A 30 mL acetonitrile solution of 5-(4-(bis(4-methoxyphenylamino)styryl)thiophen-2-yl)-2-carbaldehyde (360 mg, 0.08 mmol), cyanoacetic acid (102 mg, 0.16 mmol), and piperidine (1.7 mg, 0.02 mmol) was refluxed for 4 h under nitrogen atmosphere. Purification by extraction (petroleum ether and aq HCl (0.1 M)) and filtration of the formed solid yielded the product as a dark red solid, D9 (283 mg, 68%), mp 223.5−224.4 °C. ^{1}H NMR (500 MHz, d_6-DMSO): δ 8.42 (s, 1H), 7.91 (d, J = 4.10 Hz, 1H), 7.47 (d, J = 8.86 Hz, 1H), 7.37−7.29 (m, 2H), 7.16 (d, J = 16.04 Hz, 1H), 7.11−7.05 (m, 4H), 6.97−6.91 (m, 4H), 6.70 (d, J = 8.85 Hz, 2H), 3.75 (s, 6H). ^{13}C NMR (125 MHz, d_6-DMSO): 163.7, 156.2, 153.1, 149.0, 146.3, 141.4, 139.2, 133.0, 132.8, 128.2, 127.2, 126.9, 126.2, 117.9, 117.6, 116.6, 114.9, 96.7, 55.2. HR-MS (TOF MS ESI) *m/z*: 531.1349 [M + Na^+]. Calcd for $C_{23}H_{17}NNaOS$ (M + Na^+): 531.1355.

4,4′-Bis(*N*,*N*-(4,4′-dimethoxydiphenylamino))benzophenone. A mixture of 4,4′-bis(amino)benzophenone (1.16 g, 5.54 mmol), copper powder (2 g, 32 mmol), K_2CO_3 (9.06 g, 65 mmol), 18-crown-6 (100 mg), and iodoanisol (20.5 g, 109 mmol) was heated to reflux at 188 °C under nitrogen atmosphere with stirring for 60 h. The reaction mixture was allowed to cool to ambient temperature and was dissolved in DCM. The solution was washed with distilled water, and the organic phase was dried with $NaSO_4$ and concentrated by evaporation. Column chromatography (10% DCM in petroleum ether) yielded the product as a yellow solid (1.95 g, 56%). ^{1}H NMR (500 MHz, d_6-acetone): δ 7.60 (d, J = 8.9 Hz, 4H), 7.08 (d, J = 9.0 Hz, 8H), 6.97 (d, J = 9.0 Hz, 8H), 6.78 (d, J = 8.9 Hz, 4H). ^{13}C NMR (125 MHz, d_6-acetone): 194.0, 159.2, 154.1, 141.2, 133.1, 130.8, 129.9, 118.1, 116.893, 56.8. MS (APCI-ES) *m/z*: 637.3 [M + H]$^+$.

3-(5-Bis(4,4′-dimethoxydiphenylamino)styryl)thiophen-2-yl). To a stirred solution of 4,4′-bis(*N*,*N*-(4,4′-dimethoxydiphenylamino))benzophenone (0.24 g, 0.378 mmol) and THF (50 mL), NaH (20.5 mg, 0.529 mmol) was added, and the mixture was cooled to 0 °C over 30 min. Diethyl thiophenephosphonate (106 mg, 0.378 mmol) in THF (10 mL) was added dropwise, and the solution was kept at 0 °C for 1 h. The reaction mixture was refluxed and stirred under nitrogen atmosphere for 12 h. The reaction was quenched with EtOH. Ether/water extraction, followed by solvent evaporation and column chromatography over silica gel (20% DCM in petroleum ether), yielded a yellow oil (0.242 g, 89%). ^{1}H NMR (500 MHz, d_6-acetone): δ 7.28 (s, 1H), 7.20 (d, J = 8.9 Hz, 2H), 7.18 (d, J = 5.2 Hz, 1H), 7.11 (d, J = 9.0 Hz, 4H), 7.04 (d, J = 9.0 Hz, 4H), 6.99 (m, 5H), 6.90 (m, 9H), 6.77 (d, J = 8.8 Hz, 2H), 3.78 (s, 12H). ^{13}C NMR (125 MHz, d_6-acetone): 166.9, 166.7, 159.3, 158.7, 152.5, 151.3, 151.0, 149.8, 144.2, 141.7, 141.4, 138.9, 137.8, 137.3, 137.1, 136.4, 136.2, 131.3, 129.9, 129.1, 125.2, 65.3. MS (APCI-ES) *m/z*: 717.4 [M + H]$^+$.

3-(5-Bis(4,4′-dimethoxydiphenylamino)styryl)thiophen-2-yl)-2-carbaldehyde. 3-(5-Bis(4,4′-dimethoxydiphenylamino)styryl)thiophen-2-yl) (0.242 g, 0.338 mmol) was dissolved in DMF and cooled to −78 °C. The mixture was evacuated and kept under nitrogen atmosphere. To the mixture, $POCl_3$ (0.34 g, 0.419 mmol) was added dropwise. The reaction mixture was allowed to warm to 0 °C, whereupon it turned red. The mixture was heated to 50 °C for 3 h. The reaction mixture was cooled to ambient temperature and quenched by aq HCl (0.1 M, 100 mL). The solution was washed with brine/ether. The organic phase was dried with $NaSO_4$, and solvent removal followed by column chromatography (10% petroleum ether in DCM) yielded the product as a dark orange oil (166 mg, 59%). ^{1}H NMR (500 MHz, d_6-acetone): δ 9.82 (s, 1H), 7.71 (d, J = 3.9 Hz, 1H), 7.39 (s, 1H), 7.28 (d, J = 9.0 Hz, 2H), 7.20 (d, J = 3.9 Hz, 1H), 7.15 (d, J = 9.0 Hz, 4H), 7.08 (d, J = 8.9 Hz, 4H), 7.04 (m, 4H), 6.93 (m, 9H), 6.79 (d, J = 8.9 Hz, 2H), 3.79 (s, 12H). ^{13}C NMR (125 MHz, d_6-acetone): 184.7, 158.6, 158.1, 153.3, 151.5, 151.1, 146.7, 144.4, 142.8, 142.0, 138.1, 134.0, 132.4, 131.4, 129.8, 129.1, 128.4, 123.9, 120.5, 119.6, 116.7, 56.7. MS (APCI-ES) *m/z*: 744.4 [M + H]$^+$.

3-(5-Bis(4,4′-dimethoxydiphenylamino)styryl)thiophen-2-yl)-2-cyanoacrylic acid (D11). A 30 mL acetonitrile solution of 3-(5-bis(4,4′-dimethoxydiphenylamino)styryl)thiophen-2-yl)-2-carbaldehyde (20 mg, 0.027 mmol), cyanoacetic acid (5 mg, 0.059 mmol), and piperidine (0.85 mg, 0.01 mmol) was refluxed for 4 h under nitrogen atmosphere. Purification by extraction (petroleum ether and aq HCl (0.1 M)) and filtration of the formed solid yielded the product as dark red solid, D11 (19 mg, 87%), mp 220.5−221.5 °C. ^{1}H NMR (500 MHz, d_6-DMSO): δ 8.28 (s, 1H), 7.76 (d, J = 4.15 Hz, 1H), 7.39 (s, 1H), 7.23 (d, J = 4.18 Hz, 1H), 7.22−7.17 (m, 6H), 7.07−7.03 (m, 1H), 6.98−6.90 (m, 10H), 6.81 (d, J = 8.65 Hz, 1H), 6.69 (d, J = 8.94 Hz, 1H), 3.74 (s, 12H). ^{13}C NMR (125 MHz, d_6-DMSO): 156.0, 155.9, 149.0, 148.6, 139.7, 139.4, 134.7, 131.9, 130.1, 129.9, 128.2, 127.9, 127.4, 126.9, 118.8, 118.0, 117.5, 114.9, 114.8, 55.1, 55.1. HR-MS (TOF MS ESI) *m/z*: 834.2608 [M + Na^+]. Calcd for $C_{23}H_{17}NNaOS$ (M + Na^+): 834.2608.

Acknowledgment. We acknowledge the Swedish Reasearch Council, Swedish Energy Agency, and the Knut and Alice Wallenberg Foundation for financial support and the Korea Foundation for International Cooperation of Science & Technology through the Global Research Laboratory (GRL) Program funded by the Ministry of Science and Technology. F.D.A. thanks MIUR (FIRB 2003: Molecular compounds and hybrid nanostructured materials with resonant and nonresonant optical properties for photonic devices) and CNR (PROMO 2006) for financial support. We also thank Mr. Lien-Hoa Tran (Stockholm University) for the HR-MS measurements.

Supporting Information Available: Complete ref 22. This material is available free of charge via the Internet at http://pubs.acs.org.

JA800066Y

(33) Spraul, B. K.; Suresh, S.; Sassa, T.; Herranz, M. A.; Echegoyen, L.; Wada, T.; Perahia, D., Jr *Tetrahedron Lett.* **2004**, *45*, 3253–3256.